AD-A101 406 FOREIGN TECHNOLOGY DIV WRIGHT-PATTERSON AFB OH F/G 20/4
AN ANALYSIS OF A LAMINAR BOUNDARY LAYER IN HIGH-ENTHALPY NOZZLE--ETC(U)
JUN 81 Z LU
UNCLASSIFIED FTD-ID(RS)T-0120-81 NL

END
DATE FILMED
7 81
DTIC

FTD-ID(RS)T-0120-81

FOREIGN TECHNOLOGY DIVISION

AN ANALYSIS OF A LAMINAR BOUNDARY LAYER IN HIGH-ENTHALPY NOZZLE FLOWS

by

Lu Zhi-yun

EDITED TRANSLATION

(14) FTD-ID(RS)T-0120-81 (11) 3 June 1981

MICROFICHE NR: FTD-C-81-00490

(6) AN ANALYSIS OF A LAMINAR BOUNDARY LAYER IN HIGH-ENTHALPY NOZZLE FLOWS,

By: (10) [redacted] Zhi-yun LU (12) 191

English pages: 17

Source: (21) Acta Mechanica Sinica, No. 4, 1980, pp. 344-355

Country of origin: (USSR)

Translated by: SCITRAN
F33657-78-D-0619

Requester: FTD/TQTD

Approved for public release; distribution unlimited.

Accession For	
NTIS GRA&I	☒
DTIC TAB	☐
Unannounced	☐
Justification	
By	
Distribution/	
Availability Codes	
Dist	Avail and/or Special
A	

PREPARED BY:

TRANSLATION DIVISION
FOREIGN TECHNOLOGY DIVISION
WP-AFB, OHIO.

AN ANALYSIS OF A LAMINAR BOUNDARY LAYER IN HIGH-ENTHALPY NOZZLE FLOWS

Lu Zhi-yun
(Institute of Mechanics, Academia Sinica)

Abstract

This paper presents a simple formula for calculating the displacement thickness, momentum thickness and physical thickness of a laminar boundary layer in high-enthalpy flows in conic nozzles at hypersonic Mach numbers. The inviscid flow upstream of the throat is assumed to be in chemical and vibrational equilibrium, and downstream of the throat the flow is frozen. The present expressions for δ^*, θ and δ are given as explicit functions of the geometric dimensions of the nozzle and the parameters of the inviscid flow field at the throat and at the point considered, instead of an integral expression. Therefore, it is particularly suitable for the design of this kind of nozzle. Comparison between the result from the present formula and published experimental data shows that the agreement is satisfactory.

Symbols

a	speed of sound
A	cross-sectional area of the nozzle
$\bar{A}$	constant in equations (10) and (17)
$\bar{B}$	constant in equations (10) and (17)
C	constant in equations (17) and (18)

D diameter of the nozzle

U velocity component in the x-direction, equation (5)

v velocity component in the y-direction

V velocity component in the Y-direction, equation (5)

x coordinate along the nozzle wall

y coordinate perpendicular to the nozzle wall

X transformed coordinate, equation (2)

E_o constant, equation (14)

$f(M_e, r_1)$ function, equation (15)

$\bar{f}(M_e, r_1)$ asymptotic function of $f(M_e, r_1)$

h static enthalpy

H total enthalpy, $H = h + \frac{u^2}{2}$

H_{tr} shape factor, $H_{tr} = \delta_{tr}^*/\theta_{tr}$

k_o constant, equation (3)

k, k_1 constant equation (14)

l shearing stress parameter, $l = \frac{\theta_{tr}}{U_e}(U_e)_w$

M Mach number

n pressure gradient correlation coefficient, in reference [3]

$\tilde{n}$ pressure gradient correlation coefficient, equation (7)

N momentum parameter, equation (10)

p static pressure

P_r Prandtl number

r radial distance of a point inside the boundary layer from the axis nozzle

r* radius of the nozzle at the throat

R curvature factor, equation (5)

s enthalpy function, equation (8)

T static temperature

u velocity component in x-direction

Y transformed coordinate

z compressibility factor

α semi-conical angle of the divergent part of the nozzle
β pressure gradient parameter, reference [3]
γ specific heat ratio
γ_{is} isentropic exponent
δ boundary layer thickness
δ^* displacement thickness of the boundary layer
η integrated value in Table 1
θ momentum thickness
κ constant, equation (7)
λ Sutherland's viscosity law coefficient, equation (3)
μ viscosity coefficient
ν kinematic viscosity coefficient
ρ_0 constant, equation (7)

ξ area ratio of the nozzle $\xi = A/A^* = (r/r^*)^2$
ρ density
φ semi-conical angle of the convergent part of the nozzle

$\varphi_1(\xi_0)$ function, equation (20)
$\varphi_2(M_e, \gamma_f)$ function, equation (21)
$\varphi_3(M_e, \gamma_f)$ function, equation (22)
ψ stream function

Subscripts:

o stagnation value of the inviscid flow
e parameter at the outer edge of the boundary layer
eq value of the equilibrium flow
f value of the frozen flow
W value at the nozzle wall
tr(X,Y) value at the coordinates
* value at the throat

Whenever the coordinate variables x, y, X, Y appear as subscripts, a partial derivative with respect to that variable is implied.

I. INTRODUCTION

For the theoretical analysis of a boundary layer in high-enthalpy nozzle flow at hypersonic Mach number, only approximation methods are applicable. Until now, only numerical integration for specified stagnant conditions, geometrical dimensions and wall temperature could be done by means of sophisticated computers [1,2]. The calculation is complicated, and the results obtained by different approximation methods are usually quite different from each other [3-8]. Because of the dissimilarity of the problem and the shortage of satisfactory modifying factors, the computed results of specific nozzle shape and stagnant parameter F cannot be applied directly to another nozzle with different parameters. On the other hand, the "low density" caused by the "high enthalpy" and "high Mach number" makes the boundary layer region inside the nozzle even larger than the inviscid flow region. This means that a very accurate calculation of the displacement thickness and boundary layer thickness is absolutely required.

It was not until 1969 that Petrie [9] did some experimental investigations on high enthalpy laminar boundary layer and presented a systematic evaluation to decide which theoretical method is the most desirable. He utilized electro-beams and pressure probes to investigage the boundary layer profile inside a nozzle flow of air with stagnant parameters P_o = 1 atmosphere, T_o = 5000 K, and discovered that all theoretically computed values for δ^* are higher than the experimentally monitored value. The Cohen-Reshotko [3] method was found to have the slightest deviation, sometimes only 4% higher. Since then, this method has been more widely applied for the computation of a high enthalpy laminar boundary layer with specified nozzle parameters [14]. However, it is very difficult to apply the method in the practical design of high enthalpy nozzles. This is because the integral factor in the equation is expressed in terms of the integral form of the inviscid flow parameters of the entire nozzle flow: to calculate n, the outer edge parameter of the boundary layer must be integrated numerically from the stagnation point at the nozzle entrance to all the points at the

considered cross-section of the nozzle, and, in the course of the design, all calculations have to be repeated along with more than five iterations for a single variation of any of the nozzle inlet parameters p_o, H or geometrical parameters $\varphi, \sigma, r^*, \xi_s$ and A/A^*.

Utilizing the fact that high-enthalpy nozzle flow at hypersonic Mach numbers is generally characterized by an inviscid flow in equilibrium upstream of the throat and a chemically and vibrationally frozen flow downstream of the throat, starting from the momentum integral equation for an axial-symmetric boundary layer, modifying the definition for $\bar{n}$ downstream of the throat, applying the linearized approximation of favorable pressure gradient universal relation similar to those in [3], [9], [11] and [12], employing the Mach number M as the integration variable, using a continuous function, partial asymptotic approach method for the integral function, and specifying the condition that the "cold wall" (being a high-enthalpy ground simulation wind tunnel) has universality, much simpler expressions for $\bar{n}$, θ, δ^* and δ are derived in this paper.

These expressions contain explicit functional forms of the geometric variables of the nozzle, parameters at the throat and at the cross section. Hence, tedious numerical integration is avoided.

II. GOVERNING EQUATIONS AND BASIC ASSUMPTIONS

The region downstream of the throat is axi-symmetric, steady frozen gas flow. The boundary layer equations are written in the form suggested by Probstein, et al [13]:

$$\left.\begin{aligned} &\frac{\partial}{\partial x}(\rho u r) + \frac{\partial}{\partial y}(\rho v r) = 0 \\ &\rho u \frac{\partial u}{\partial x} + \rho v \frac{\partial u}{\partial y} = -\frac{\partial p}{\partial x} + \frac{1}{r}\frac{\partial}{\partial y}\left(\mu r \frac{\partial u}{\partial y}\right) \\ &\rho u \frac{\partial H}{\partial x} + \rho v \frac{\partial H}{\partial y} = \frac{1}{r}\left\{\frac{\partial}{\partial y}\left(\frac{\mu r}{\mathrm{Pr}}\frac{\partial H}{\partial y}\right) + \frac{\partial}{\partial y}\left[\mu\left(1-\frac{1}{\mathrm{Pr}}\right) r u \frac{\partial u}{\partial y}\right]\right\} \end{aligned}\right\} \qquad (1)$$

in which $H = h + \frac{u^2}{2}$. Introducing the Stewartson [14] and Mangler [15] transformation:

$$\left.\begin{aligned} X &= \int_0^x \lambda \frac{a_e}{a_0} \frac{\rho_e}{\rho_0} r_w^2 dx \\ Y &= \frac{a_e}{a_0} \int_0^y \frac{\rho}{\rho_0} r dy \end{aligned}\right\} \tag{2}$$

where λ is determined by the viscosity law:

$$\left.\begin{aligned} &\frac{\mu}{\mu_0} = \lambda \frac{T}{T_0} \\ &\lambda = \sqrt{\frac{T_0 + k_0}{T_w + k_0}} \sqrt{\frac{T_w}{T_0}}; \quad k_0 = 110\text{K} \end{aligned}\right\} \tag{3}$$

The stream function is defined by:

$$\phi_x = -\frac{\rho}{\rho_0} vr; \qquad \phi_y = \frac{\rho}{\rho_0} ur. \tag{4}$$

The following relations are also introduced:

$$U = \phi_Y = \frac{a_0}{a_e} u; \quad V = -\phi_X; \quad R = \left(\frac{r}{r_w}\right)^2 = \left(1 - \frac{Y \cos\alpha}{r_w}\right)^2. \tag{5}$$

Substituting equations (2) to (5) into (1) and simplifying,

$$\left.\begin{aligned} &U_X + V_Y = 0 \\ &UU_X + U_Y V = U_e U_{eX} \left(\frac{u^2/2 + a^2/(\gamma-1)}{u_e^2/2 + a_e^2/(\gamma_e - 1)}\right) + \nu_0 \frac{\rho_0}{p_e^*} \frac{\rho_e^*}{\rho_0} \frac{T_e^*}{T_0} (RU_Y)_Y \\ &UH_X + VH_Y = \left(1 - \frac{1}{\Pr}\right) \frac{a_e^2}{a_0^2} \nu_0 \frac{\rho_0}{p_e^*} \frac{\rho_e^*}{\rho_0} \frac{T_e^*}{T_0} (RUU_Y)_Y + \frac{\nu_0}{\Pr} \frac{\rho_0}{p_e^*} \frac{\rho_e^*}{\rho_0} \frac{T_e^*}{T_0} (RH_Y)_Y \end{aligned}\right\} \tag{6}$$

Now the following basic assumptions are made:

(a) The flow inside the boundary layer is also chemically vibrationally frozen. According to experimental results for the air medium, the N_2 vibrational relaxation phenomenon inside the boundary layer is extremely

weak. Hence, it can be assumed that the chemical combination is even weaker.

b) The second order effect of the lateral curvature effect is neglected. This is because the lateral curvature effect has an apparent influence on the velocity profile and the friction drag but very little influence on δ^*. Hence, $R \approx 1$ can be taken for granted.

c) $Pr \approx 1$. Since the condition of a strong, favorable pressure gradient flow at a hypersonic Mach number outside an isothermal wall is involved here, $Pr = 1$ is almost valid. Petrie [9] analyzed the velocity and temperature profiles at different Pr under the condition of large β values. The observed results by means of an electron gun show that the assumption of $P \approx 1$ is valid.

d) The pressure gradient correlation coefficient $\bar{n}$ is redefined as:

$$\bar{n} = \frac{-U'_{ex}\theta'_{tr}}{\bar{\nu}_0}; \quad \bar{\nu}_0 = \nu_0 \frac{\rho_0}{\rho_e^*}\frac{\rho_e^*}{\rho_0}\frac{T_e^*}{T_0} = \kappa\nu_0 \tag{7}$$

e) The enthalpy function is defined as:

$$s = \frac{u^2/2 + a^2/(\nu-1)}{u_e^2/2 + a_e^2/(\nu_e-1)} - 1$$

and it is assumed that:

$$s \approx \frac{H}{H_e} - 1 \tag{8}$$

III. THE SIMPLIFICATION AND SOLUTION FOR THE RELATION FOR $\bar{n}$

Under the above basic assumptions, the boundary layer momentum equation can be integrated along the Y-axis from 0 to ∞ and a momentum integral relation of exactly the same form as those given by the references [3], [9], [11] and [12] is obtained:

$$-U_e \frac{d}{dX}\left(\frac{\bar{n}}{U_{eX}}\right) = 2[\bar{n}(H_{ir}+2)+l] \tag{9}$$

The universality of this kind of differential equation for favorable pressure gradient under the condition of incompressible flow was first proved by Thwaites [11]. Later, Kochin-Loytsyanskiy [12] and Cohen-Reshotko [3] also adopted the universal relation of this form. After linear approximation, equation (9) becomes:

$$N(s_w, \bar{n}) = 2[\bar{n}(H_{ir}+2)+l] \approx \bar{A} + \bar{B}\bar{n} \tag{10}$$

Integrating, the expression for $\bar{n}$ downstream of the throat is:

$$\bar{n} = -\bar{A}U_{eX}U_e^{-\bar{B}}\left[\int_{X^*}^{X} U_e^{\bar{B}-1}dX - \frac{\bar{n}^*}{\bar{A}U_{eX}^* U_e^{*-\bar{B}}}\right] \tag{11}$$

For the region upstream of the throat, if an isentropic flow of a perfect gas of $\gamma_\infty < 1.400$ is assumed to be equivalent to the isentropic equilibrium flow, the following expression is obtained:

$$n^* = -\bar{A}U_e^{*-\bar{B}}U_{eX}^*\left[\int_0^{X^*} U_e^{\bar{B}-1}dX - \frac{n_0}{(\bar{A}U_e^{-\bar{B}}U_{eX})_{X=0}}\right] \tag{12}$$

Modifying (12) by the factor $\kappa = \frac{\rho_0}{\rho_e^*}\frac{\rho_e^*}{\rho_0}\frac{T_e^*}{T_0}$, substituting into

(11), and transforming back to the (x,y) coordinates plane, the following is obtained:

$$\bar{n} = -AM_e^{-B}\frac{dM_e}{dx}\frac{1}{r_w^2}\left(\frac{p}{p_0}\right)^{-k}\left[\frac{1}{\varepsilon}\int_0^{x^*}\left(\frac{p_e}{p_0}\right)^{k}M_e^{B-1}r_w^2dx + \int_{x^*}^{x}\left(\frac{p_e}{p_0}\right)^{k_1}M_e^{B-1}r_w^2dx + \frac{|n_0|}{\varepsilon E_0}\right] \tag{13}$$

where:

$$k = \frac{3\gamma_{es}-1}{2\gamma_{es}};\quad k_1 = \frac{3\gamma_f-1}{2\gamma_f};\quad E_0 = \bar{A}M_e^{-B}\left(\frac{dM_e}{dx}\right)_{x=0}\frac{1}{r_0^2}\left(\frac{p}{p_0}\right)^{-k}_{x=0} \tag{14}$$

For various γ_{es} upstream of the throat, the calculated values of the first integral in equation (13) are shown in Table 1. When ambient pressure p_o is varied in the range 1-5 atmospheres and H_e in the range 2000-5000 kcal/kg, the values of γ_{es} at the points upstream of the throat vary from 1.22-1.35 correspondingly. Based on Table 1, the variation of the integral is less than 2.6%. Also from an order analysis, the second integral in equation (13) is one order of magnitude higher than the first integral at hypersonic Mach number. Hence, the error of $\bar{n}$ due to variation of the value of the first integral, induced by taking different γ_{es}, is generally less than 0.35%. Therefore, any flow of perfect gas with γ_{es} between 1.22 and 1.35 can be used to simulate the equilibrium flow and calculate the value for n. Downstream of the throat, the integration variable x of the second integral in equation (14) can be transformed into $\xi = \frac{A}{A^*} = \left(\frac{r_w}{r^*}\right)^2$, by replacing the isentropic relation for a perfect gas with the isentropic relation for the chemically and vibrationally frozen flow, and by replacing the relation for the nozzle flow of perfect gas with the relation between the corresponding area ratio A/A* and M_e. Transforming ξ into M_e, the following is obtained:

$$\int_{x_0}^{x}\left(\frac{p_e}{p_0}\right)^{\frac{2\gamma_f-1}{2\gamma_f}} r_b^{\frac{1}{2}} M_e^{\bar{B}-1} dx$$

$$= \frac{r^{*\frac{1}{2}}}{2\sin\alpha}\left(\frac{a_{eq}^*}{a_f^*}\right)^{3/2}\left(\frac{p_e^*}{p_0}\right)^{\frac{2\gamma_f-1}{2\gamma_f}}\left(1+\frac{\gamma_f-1}{2}\frac{a_{eq}^{*2}}{a_f^{*2}}\right)^{\frac{7\gamma_f-5}{4(\gamma_f-1)}} \tag{15}$$

$$\times \int_{\frac{a_{eq}^*}{a_f^*}}^{M_e}\left(1+\frac{\gamma_f-1}{2}M_e^2\right)^{\frac{5-7\gamma_f}{4(\gamma_f-1)}}\left(M_e^{\bar{B}-1.5}-\frac{1}{M_e^{3.5-\bar{B}}}\right)dM_e$$

Taking $\bar{B} = 2.50$, the first term in equation (15) can be integrated for any γ_f. For the second integral function:

$$f(M_e, \gamma_f) = \left(1+\frac{\gamma_f-1}{2}M_e^2\right)^{\frac{5-7\gamma_f}{4(\gamma_f-1)}}\frac{1}{M_e}$$

$\gamma_f = 1.400$ is taken as the left end point, and different ΔM_e, $\Delta\gamma_f$ are expanded and asymptotically approached between $\gamma_f = 1.400$ and 1.5. In doing so, the asymptotic function for $f(M_e, \gamma_f)$ at different Mach numbers can be obtained:

$$\overline{f(M_e, \gamma_f)} = \begin{cases} \dfrac{1.080}{M_e} - 0.167[1 + 4.49(\gamma_f - 1.400)] & (1 \leqslant M_e \leqslant 2.5) \\ \dfrac{1.115}{M_e^{1.516+2.20(\gamma_f-1.400)}} - 0.016[1 + 6.25(\gamma_f - 1.400)] & (2.5 < M_e \leqslant 10) \\ 0 & (M_e > 10) \end{cases} \tag{16}$$

It can be proved that when $1 \leqslant M_e \leqslant 2.5$, the asymptotic error $(\bar{f} - f)/f < 2\%$. For $2.5 \leqslant M < 5$, $(\bar{f} - f)/f \approx 4.4\%$. However, the value of f has little contribution to the integral in equation (15) when $2.5 \leq M_e \leq 5$. Hence, it can be shown that the error of integration is still within 2%.

Substituting expression (16) into equation (15), and substituting the η value corresponding to $\gamma_{es} = 1.25$ along with equation (15) into (13), and applying the speed of sound relation, the differential form of Euler's equation of motion and the energy equation under chemically and vibrationally frozen flow, the following can be obtained after simplification:

$$\bar{n} = -\bar{A}\frac{\left(1+\frac{\gamma_f-1}{2}M_e^2\right)^{\frac{7\gamma_f-9}{4(\gamma_f-1)}}}{M_e^2-1}\left\{\frac{C}{\kappa}\frac{\sin\alpha}{\sin\varphi}\left[\varphi_1(\xi_0)+\frac{n_0}{C_{es}\bar{A}}\right]\right. \tag{17}$$

$$\left. + \varphi_2(M_e, \gamma_f) - \varphi_3(M_e, \gamma_f)\right\}$$

where

$$C = \left(\frac{a^*_{cs}}{a^*_f}\right)^{-3/2}\left(\frac{p^*_r}{p_0}\right)^{-\frac{3\gamma_f-1}{2\gamma_f}}\left(1+\frac{\gamma_f-1}{2}\frac{a^{*2}_{cs}}{a^{*2}_f}\right)^{\frac{5-3\gamma_f}{4(\gamma_f-1)}} \tag{18}$$

$$C_{cs} = \left(\frac{2}{\gamma_{cs}+1}\right)^{-\frac{3(\gamma_{cs}+1)}{4(\gamma_{cs}-1)}} \quad (\text{当 } \gamma_{cs} = 1.25 \text{ 时}, C_{cs} = 2.21) \tag{19}$$

$$\varphi_1(\xi_0) = 0.0163 + 0.4512 \ln \xi_0 + 0.08\xi_0^{-2} \tag{20}$$

$$\varphi_2(M_e, \gamma_f) = \frac{4}{5-3\gamma_f}\left[\left(1+\frac{\gamma_f-1}{2}M_e^2\right)^{\frac{5-3\gamma_f}{4(\gamma_f-1)}} - \left(1+\frac{\gamma_f-1}{2}\frac{a^{*2}_{cs}}{a^{*2}_f}\right)^{\frac{5-3\gamma_f}{4(\gamma_f-1)}}\right] \tag{21}$$

$$\begin{aligned}\varphi_3(M_e, \gamma_f) = {} & 1.080 \ln \frac{2.5}{(a^*_{cs}/a^*_f)} + (0.883 - 0.75\gamma_f)\left(2.5 - \frac{a^*_{cs}}{a^*_f}\right) \\ & + \frac{0.507}{\gamma_f - 1.166}\left[2.5^{-2.2(\gamma_f-1.166)} - M_e^{-2.2(\gamma_f-1.166)}\right] \\ & + (0.124 - 0.1\gamma_f)\left(M_e - \frac{a^*_{cs}}{a^*_f}\right)\end{aligned} \tag{22}$$

Further manipulation gives the solution for momentum thickness θ, displacement thickness δ^* and boundary layer thickness δ:

$$\theta = \frac{T_e}{T_w}\left[\frac{\bar{n}\nu_w}{du_e/dx}\left(1+\frac{\gamma_f-1}{2}M_e^2\right)^{-1}\right]^{1/2} \tag{23}$$

$$\delta^* = \theta\left[H_{tr} + \frac{\gamma-1}{2}M_e^2(1+H_{tr})\right] \tag{24}$$

$$\delta = \theta\left[\delta_{tr}/\theta_{tr} + \frac{\gamma_f-1}{2}M_e^2(1+H_{tr})\right] \tag{25}$$

In the above expressions, H_{tr} and δ_{tr}/θ_{tr} can be obtained by the similarity profile solution of the Falkner-Skan type flow given in reference [4]; δ^*_{tr} is determined by $\delta^*_{tr} = \int_0^\infty \left(1 - \frac{U}{U_e} + s\right) dY$; θ_{tr} is determined by the expression $\theta_{tr} = \int_0^\infty \frac{U}{U_e}\left(1 - \frac{U}{U_e}\right) dY$; δ_{tr} is the $\eta = Y\sqrt{\frac{m+1}{2}\frac{U_e}{\nu_0 X}}$ value corresponding to the incompressible plane when $U/U_e = 0.995$, and n_o is the value of n at

which $N(s_w, \bar{B}) = 0$, corresponding to the intersection point of $\beta = 1$ and s_w = constant.

In general, water-cooled copper walls are used for high-enthalpy flow nozzles in simulation wind tunnels on the ground. The wall temperature satisfies $T_w \leq 400K$. When the stagnation temperature T_o is between 2000 K and 8000 K, $-0.95 \leq \frac{T_w}{T_o} - 1 \leq -0.80$, that is, the following relation is also satisfied:

$$-1 < s_w \leq -0.80 \tag{26}$$

Now from the universal relation curve, the corresponding value of $\bar{B}$ is found to satisfy:

$$2.36 < \bar{B} \leq 2.53 \tag{27}$$

From equation (11), it can be observed that the $\bar{B}$ index inside the integral sign is cancelled by the $\bar{B}$ index preceding the integral sign. Hence, it is regarded that the variation of $\bar{B}$ will not cause a large scale variation in $\bar{n}$. Table 2 shows the difference in $\bar{n}$, θ and δ^* caused by taking $\bar{B}$ as 2.5 and 2.3, with the same nozzle parameters. Under the practical condition of a high-enthalpy cold wall, as discussed in this paper, the value of $\bar{B}$ is closer to the higher extreme of the inequality. Therefore, the true error of $\bar{n}$, θ and δ^* caused by taking $\bar{B} = 2.5$ is far smaller than those in Table 2. Besides, analyzing the data from the numerical integration of the similarity solution for the momentum integral equation, it is found that the increase in $\bar{B}$ also causes an increase of $\bar{A}$, which in turn reduces the variation of the value of $\bar{n}$. Hence, it is reasonable to take $\bar{B} = 2.50$.

IV. CONCLUSION

In the present effort, the inviscid region of the high-enthalpy nozzle flow at hypersonic Mach number upstream of the

throat is assumed to be equilibrium flow, while the region downstream of the throat is assumed to be chemically and vibrationally frozen flow. The flow within the boundary layer is also treated as chemically and vibrationally frozen flow, on the basis of a monitored data analysis of the N_2 vibrational temperature relaxation. The isentropic relation under the frozen flow condition is utilized for the outer edge of the boundary layer. The modification factor $\frac{\rho_0}{\rho_e^*}\frac{\rho_e^*}{\rho_0}\frac{T_e^*}{T_0}$ is introduced to modify the pressure gradient correlation coefficient. A linear approximation method for the favorable pressure gradient universal relation is applied, and the cold wall condition $\bar{B}$ is treated as single-valued. Under all these conditions and employing order of magnitude analysis, integral transformation, dimensionless Mach number and partial asymptotic approach method for the integral function, the explicit functional expressions for $\bar{n}$, δ^* and δ are derived.

The present investigation shows that when p_o is between 1-5 atmospheres and H_e between 2000 and 5000 kcal/kg or varies within an even greater range, the calculation of the pressure gradient correlation number $\bar{n}$ upstream of the throat can be done using $\gamma_{es} = 1.25$, or the "equivalence" of the perfect gas flow of the corresponding isentropic exponent. Although the calculation of $\bar{n}$ downstream of the throat is off by approximately 2% due to the asymptotic method for the integral function, the results at the nozzle exit calculated by the formulae presented here are still close to the experimental data after modification of the isentropic relation. For example, for air at $T_o = 5000$ K, $p_o = 1.16$ atmosphere, and at the section $D/D^* = 9$ downstream of the throat, the deviated values of θ and δ^* are corrected by 4.2% with a modification of the isentropic relation only. Table 3 lists the actual samples of the nozzle calculation, and Figure 2 shows a comparison of the results from the present analysis, the results from other theories and foreign published experimental data.

Observing the results in Table 3, it is apparent that the deviation of the calculated results for the points downstream of the throat from the experimental results is greater. This is quite natural, because the boundary condition has switched from a non-slip wall condition to a free jet flow boundary condition. This portion of the flow field should be calculated by a non-similarity method of free-shear layer [16]. The methods and the results given here are no longer applicable.

The formulae given here can be used for the boundary layer calculation of high-enthalpy hypersonic Mach number, cold constant temperature wall conical nozzles. Since common integral expressions are avoided, the calculation is much simplified. Hence, it is especially suitable for the engineering design of this kind of nozzle. Common high-enthalpy, low-density electric arc wind tunnel nozzles and low-density, low-temperature plasma flow nozzles with a water-cooled copper wall also belong to this category.

The author would like to express his gratitude toward Mr. Yang-gwei Bian for his advice and assistance.

REFERENCE

[1] Быркин, А. Г., *Ж. Вычисл. Матем. и Матем. физ.* **10**, 1(1970), 124—131.
[2] David, L. Whitfield and Chark H. Lewis, *J. of Spacecraft and rockets*, 7 (1970), 462.
[3] Cohen, C. B. and Reshotko, E., NACA Report, 1294 (1956).
[4] Luce, R., Gregorek, G. M. and Lee, J. D., USAF ARL Report, 65—112.
[5] Bechwith, I. E., Cohen, C. B., NASA TND-625 (1961).
[6] Clutter, D. W., Smith, A. M. O., Douglas Report, LB 31088 (1964).
[7] Smith, A. M. O., Clutter, D. W., *AIAA. J.*, 4(1965), 639.
[8] Jaffe, N. A., Lind, R. C., Smith, A. M. O., *AIAA. J.* 9(1967), 1563.
[9] Petrie, S. L., NASA-CR-96152 April (1968).
[10] James, T. Van Kuren. AFFDL-TR-74-59.
[11] Thwaites, B., *Aero. Quarterly*, 1, 11(1949), 245—280.
[12] Кочин, Н. Е. и Лонцянский, Л. Г., *ДАН СССР*. **36**, 9(1942).
[13] Probstein, R. F., Elliott, D., *J. Aeronaut. Sci.* **23**(1956), 208.
[14] Stewartson, K., *Proc. Roy. Soc. (London), Ser. A* **200**, (1949), 84—100.
[15] Mangler, W., *Zeitschr. f. Angew. Math. and Mech.* **28**(1948), 97.
[16] Lykoudis, P. S., *AIAA. J.*, 4(1966), 577.

TABLE 1.

$\frac{2\sin\varphi}{r^{*2}}\int_0^{x^*}\left(\frac{p_c}{p_0}\right)^{\bar{A}_1}M_c^{\bar{B}-1}r_w^2\,dx$ WHEN $\bar{B}$ = 2.50

r_{w_1}	$\eta=\frac{2\sin\varphi}{r^{*2}}\int_0^{x^*}\left(\frac{p_c}{p_0}\right)^{\bar{A}_1}M_c^{\bar{B}-1}r_w^2\,dx$
1.222	$0.0168+0.4537\ln\bar{x}_c+0.08\bar{x}_c^{-1}$
1.250	$0.0163+0.4512\ln\bar{x}_c+0.08\bar{x}_c^{-1}$
1.286	$0.0153+0.4486\ln\bar{x}_c+0.08\bar{x}_c^{-1}$
1.300	$0.0148+0.4478\ln\bar{x}_c+0.08\bar{x}_c^{-1}$
1.400	$0.0114+0.4401\ln\bar{x}_c+0.08\bar{x}_c^{-1}$

TABLE 2.

THE EFFECT OF $\bar{A}$ AND $\bar{B}$ ON THE RESULTS

D^* = 8mm, α = 7.5°, φ = 22.5°, r_0/r^* = 6, r_1 = 1.455

M_e	1)序 号	$\bar{B}$	$\bar{A}$	$\bar{n}_1/\bar{n}_2$	θ_1/θ_2	δ_1^*/δ_2^*
7	1	2.50	0.361	0.902	0.950	0.968
	2	2.30	0.327			
5	1	2.50	0.361	0.885	0.941	0.958
	2	2.30	0.327			
2.5	1	2.50	0.361	0.840	0.916	0.946
	2	2.30	0.327			

1) sequence number;

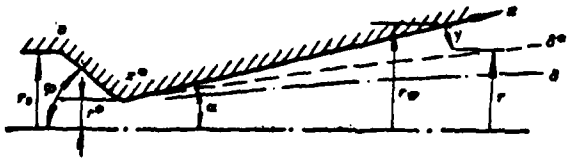

Figure 1. Geometric dimensions of the nozzle.

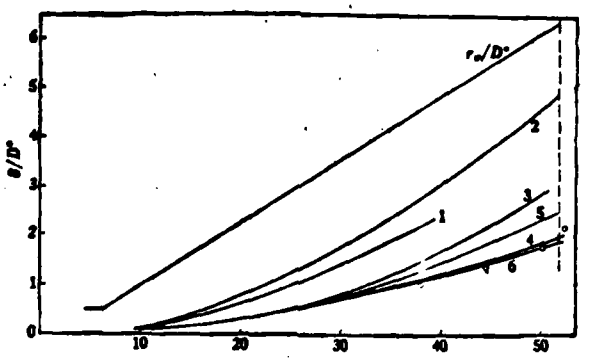

Air $T_0 = 500°K$
$\rho_0 = 1.16aTM$
$T_w = 350°K$
$\gamma = 1.455$
$Z = 1.180$

Figure 2. The growth of boundary layer displacement thickness δ^* : o Experimental data, 1) Pohlhausen energy integral; 2) Pohlhausen momentum integral; 3) Beckwith-Cohen method; 4) Cohen-Reshotko method; 5) modified method, reference [1]; and 6) equations 17 - 25 given here.

表3 排挤厚度 δ^* 的最后结果比较 1

$D^* = 8mm$, $\alpha = 7.5°$, $\varphi = 22.5°$, $r_0/r^* = 6$, $\gamma_1 = 1.455$, $s_w = -0.93$

	x/D^*	38.1	44.5	50.1	52.4
2 排挤厚度（厘米）	实验测量值 3	0.845	1.14	1.42	1.72
	Cohen-Reshorko 方法的 IBM7094 计算机结果 4	0.903	1.19	1.47	1.58
	本文公式(16)等 5	0.880	1.17	1.41	1.54

1) Table 3 Comparison of Final Results With an Exclusion thickness of δ^*

2) Exclusion thickness (cm); 3) Experimentally determined values
4) Results with an IBM 7094 computer using the Cohen-Resnorko method;
5) Formula (16), and so on, as found in this article;

AN ANALYSIS OF LAMINAR BOUNDARY LAYER IN HIGH ENTHALPY NOZZLE FLOWS

Lu Zhi-yun

(Institute of Mechanics, Academia Sinica)

Abstract

This paper presents a simple formula for calculating the displacement thickness, momentum thickness and physical thickness of laminar boundary layer in high enthalpy flows in conic nozzles at hypersonic Mach numbers. The inviscid flow upstream of the throat is assumed to be in chemical and vibrational equilibrium and downstream of the throat the flow is frozen. The present expressions for δ^*, θ and δ are given as explicit functions of the geometric dimensions of the nozzle and the parameters of the invicid flow field at the throat and at the point considered, instead of an integral expression. Therefore it is particularly suitable for the design of this kind of nozzle. Comparison between the result from the present formula and published experimental data shows that the agreement is satisfactory.